ORIGINAL ARTICLE

Phytochemicals and Proteomic Profiling of Ethyl Acetate of *M. micrantha* Extract Treated Hypercholesterolemic Rats

Azlinda Ibrahim[1], Nurul Husna Shafie[1,2], Norhaizan Mohd Esa[1], Siti Raihanah Shafie[1], Hasnah Bahari[3], Nurul Hayati Mohamad Zainal[3]

[1] Department of Nutrition, Faculty of Medicine and Health Sciences, Universiti Putra Malaysia, 43400 UPM Serdang, Selangor, Malaysia
[2] Laboratory of UPM-MAKNA Cancer Research, Institute of Bioscience, Universiti Putra Malaysia, 43400 UPM Serdang, Selangor, Malaysia
[3] Department of Human Anatomy, Faculty of Medicine and Health Sciences, Universiti Putra Malaysia, 43400 UPM Serdang, Selangor, Malaysia

ABSTRACT

Introduction: *Mikania micrantha* possess potent anti-hypercholesterolemic properties. However, the phytochemicals of *M. micrantha* and protein regulation that led to its hypocholesterolemia effects are limited. The aim of this study is to investigate the phytochemicals and proteomic profiling of liver samples from hypercholesterolemic rats that were treated with *M. micrantha* extract. **Materials and methods:** The identification of phytochemicals in the ethyl acetate of *M. micrantha* stem (EAMMS) extract was conducted through the liquid chromatography quadrupole time-of-flight mass spectrometry (LC-QToF-MS). The rats were divided into two distinct groups: a normal group (NC) and a group induced with hypercholesterolemia, both of which were observed for an initial duration of four weeks. Following the completion of the fourth week of the induction period, the rats were divided into five groups: 1% high cholesterol diet (HCD), 1% HCD + Simvastatin (10 mg/kg of body weight (BW)), 1% HCD + EAMMS (50 mg/kg/BW), 1% HCD + EAMMS (100 mg/kg/BW) and 1% HCD + EAMMS (200 mg/kg/BW) for another 4 weeks of treatment periods. The LC-MS/MS analysis was conducted on liver tissue to identify differentially expressed proteins. **Results:** The phytochemicals were identified in the EAMMS extract, including theobromine, ishwarol, pheophorbides, and dihydromikanolide. In association with hypercholesterolemia, a total of 26 differentially expressed proteins were identified. Among these proteins, nine proteins exhibited elevated levels, whereas 17 showed downregulation, which mainly involved in lipid metabolism pathway. **Conclusion:** Overall, these results provide understanding on the molecular targets of EAMMS extract, which could be used for further study on the putative anti-hypercholesterolemic properties.
Malaysian Journal of Medicine and Health Sciences (2024) 20(4): 114-123. doi:10.47836/mjmhs20.4.15

Keywords: *Mikania micrantha*, Anti-hypercholesterolemia, Proteomic, Phytochemicals, LC-MS/MS

Corresponding Author:
Nurul Husna Shafie, PhD
Email: nhusnashafie@upm.edu.my
Tel : +603-97692470

INTRODUCTION

Hypercholesterolemia is described as a metabolic anomaly where the level of plasma low density lipoprotein (LDL) cholesterol is elevated (1). Numerous cardiovascular disorders, such as atherosclerosis, cerebral paralysis, and myocardial infarction, as well as inflammation and cancer, have been linked to hypercholesterolemia (2,3). Over the past several decades, products of botanical origin have been regarded to possibly contain therapeutic agents which are novel in the treatment of hypercholesterolemia as these plants may be the source of secondary metabolites, which are bioactive substances with different structures, including alkaloids, flavonoids, phenolic acids, resin, tannins, terpenoids, saponins, steroids, and others (4). Besides, plants are gaining immense popularity all over the world as consumers are becoming more inclined towards natural and safe products that are also relatively lower in toxicity, easily available, cost-effective, and most significantly, have less adverse consequences (4,5) than the synthetic drugs such as statin group, simvastatin that are asymptomatic increases in liver enzymes such as liver transaminases, AST and ALT (6); as well as caused myopathy (7).

Mikania micrantha Kunth is a plant that is native to tropical central and southern America. This species has spread and is prevalent in the Pacific as well as

in South-east Asian countries (8,9). *M. micrantha* is known as Bitter Vine, American Rope, mile-a-minute, 'Sembung rambat' (Indonesia) and 'Selaput tunggul' in Malaysia (10-12). *M. micrantha* is traditionally used as a remedy for the treatment of maladies such as jaundice, dysentery, respiratory ailments, stomach aches and rheumatism. Parts of this perennial creeper are also made into concoctions and consumed as folk medicine in addressing hypertension, diabetes, and hypercholesterolemia (13,14). Numerous health advantages associated with *M. micrantha* have been documented in the literature, encompassing antioxidant (15), anti-diabetic (16), anti-cancer (17,18), antiproliferative (19), anti-dermatophytic (20), and anti-inflammatory (21) properties. In addition, the medicinal properties of this species are linked to the abundance of its inherent chemical components namely terpenoid, flavonoid, alkaloids, and vitamins (14,15,20,22).

It has been shown the potential anti-hypercholesterolemic effects of the ethyl acetate of *M. micrantha* stems extract and showed the potential inhibitory effects on the HMG-CoA reductase and acetyl-CoA acetyltransferase 2 enzymes (6). However, the data on protein targets are limited and its mechanism of action as an anti-hypercholesterolemic remains unknown. Besides, the phytochemical constituents of *M. micrantha* extracts that may potentially contribute to the anti-hypercholesterolemia properties were limited.

At present, liquid chromatography quadrupole time-of-flight mass spectrometry (LC-QToF-MS) is the method of choice for its reliable screening and identification of compounds as well as the quantification of both unknown and targeted compounds in the sample while continuously expanding the database (23). Many studies have been conducted in recent years that have successfully used proteomics to identify potential prognostic and diagnostic markers, understanding protein interaction networks and metabolic rearrangements leading to disease phenotype disorders, as well as comprehending disease mechanisms for various types of CVD, including hypercholesterolemia (24-25). The proteomic data on pathway enrichment and protein interaction analyses, give shed light on probable underlying biological mechanisms and pathways connected to hypercholesterolemia, and the information on the phytochemical constituents will also support the underlying mechanism. Therefore, we aimed to investigate the changes in the liver proteome profiling in EAMMS-treated hypercholesterolemia-induced rats and the identification of bioactive compounds that presence in this plant extract.

MATERIALS AND METHODS

Sample collection and preparation

Mikania micrantha was collected from Negeri Sembilan, Malaysia. Fresh *M. micrantha* stems were chosen, washed, and dried for 72 h in a ventilated drying oven. The dried samples were grinded by a fine mesh sieve into fine powder form and were stored at -20°C prior to further extractions.

Extraction of *M. micrantha*

The ethyl acetate (100%) (LC-MS grade) was used for making extracts. A 25 g of the dried powdered stems of *M. micrantha* were immerged in 250 mL of pure ethyl acetate. Then, the mixture was homogenized on an orbital shaker at 100 rpm for three days at ambient temperature (24°C). Next, the extract was filtered with a Whatman filter paper No. 1 and then concentrated using rotary vacuum evaporator at 100 rpm and 48°C. The extract was left in laminar flow to ensure the solvents are removed completely and dried extract obtained. All the extracts were stored at -20°C prior to analysis (15).

Identification of phytochemicals in the ethyl acetate of *M. micrantha* stem (EAMMS) extract

The identification of phytochemicals in the ethyl acetate of *M. micrantha* stem (EAMMS) extract was employed using LC-QToF-MS analysis. The crude sample (1 mg) was dissolved in 1 mL of methanol. LC-QToF-MS analysis was utilising the Agilent 1290 Infinity LC system and Agilent 6530 Accurate-Mass QToF mass spectrometer. The column that was used is an Agilent Zorbax Eclipse XDB-C18 narrow-bore column (150 mm length x 2.1 mm internal diameter, 3.5-micron particle size) with column temperature at 25 °C, autosampler temperature at 4 °C, flowrate at 0.5 mL/mins. The mobile phases used were 0.1% v/v formic acid in water and 0.1% v/v formic acid in acetonitrile. The positive and negative ionisation modes were deployed for an ESI- QToF-MS analysis. The fragmentor employed a voltage of 125 V and a drying gas temperature of 300°C. The drying gas flow was set at 10 L/min, and 10 µL of the sample was injected from the auto-sampler each time. For MS condition, the source of ESI ion polarity was set at negative and positive, and the mass range was from 100 – 3200 m/z. The raw data was processed with Molecular Feature Extraction with Extraction algorithm set at small molecule (chromatographic), peak filters with peak height ≥100 counts and compound filters to only look for compound with absolute height ≥5000 counts and relative height ≥2.5%. The data on bioactive compounds, precursor ions, mode and spectrum activity were validated using natural product databases, such as PubChem (https://pubchem.ncbi.nlm.nih.gov/) and Chem Spider (http://www.chemspider.com/).

Animal handling and sampling

Male Sprague Dawley rats (150-200 g weight) were acclimatised for a week with standard food and tap water *ad libitum*. The rats were accommodated in a controlled environment (temperature: 24 ± 2°C; relative humidity: 55 ± 4%; dark/light circle: 12-hour). This facility is located at the Animal House, which is part of the Faculty of Medicine and Health Sciences at Universiti Putra

Malaysia. The animal study received approval from the Institutional Animal Care and Use Committee (IACUC) at Universiti Putra Malaysia (UPM) under the reference number UPM/IACUC/AUP-R081/2017. The rats were divided into six groups using random assignment, with each group consisting of six rats. First group, designated as the normal control, was provided with a standard diet over a period of eight weeks. Rats in groups 2 to 6 were subjected to oral administration of a high cholesterol diet (1% HCD) for eight weeks of duration of the study. At the fifth week, rats in groups 3-6 were fed a high cholesterol diet and subsequently administered EAMMS extract at low (50 mg/kg), medium (150 mg/kg), or high dose (200 mg/kg) as well HMG-CoA reductase inhibitors, or simvastatin (10 mg/kg) for four weeks during the treatment phase. At the end of experimental period, rats were anesthetized using ketamine (100 mg/kg) and xylazine (10 mg/kg). Then, the blood and tissues were collected and stored until the point of analysis.

Protein extraction and digestion

Each liver sample (10 mg) was cut into tiny pieces and then minced into tiny particles. Subsequently, samples were washed with ultrapure water until the tissue fluid became clear. The cells were lysed using a homogenizer on ice. The cell lysate was then be subjected to centrifugation to remove the cell debris (10 minutes, at 1000 g, 4°C) (26). In order to decrease the occurrences of protein denaturation, the entire process was carried out at a temperature of 4°C on ice. The isolated proteins were kept at a temperature of -80°C.

The Rapid Digestion - Trypsin kit, manufactured by Promega Corporation in Fitchburg, USA, was utilised for protein digestion in accordance with the instructions provided by the manufacturer. Briefly, 50 µL of protein substrate was quickly added to 150 µL of Rapid Digest Buffer, then incubated for 1 hour at 70 °C after adding 3.0 µL of Rapid Trypsin (1 µg/L). To stop the reaction from continuing, 0.5 µL of formic acid was subsequently added to the mixture. The samples were then cleaned up via a Pierce C18 Spin Column. Prior to LC-MS/MS analysis, the acquired samples were filtered using a 0.22 µm syringe filter and kept at -80°C.

Proteomic analysis

The LC-MS/MS analysis was conducted following a protocol (27). The digested peptides (1 µL; 4°C) were loaded into an Agilent C18 300 E Large Capacity Chip column that was equilibrated with 0.1% formic acid in ultrapure water (solution A). The peptides were eluted from the column with 90% acetonitrile in 0.1% formic acid in water (solution B). Solvent A was observed to have a flow rate of 4 µL/min, while solvent B exhibited a flow rate of 0.5 µL/min. The quadrupole time-of-flight (QToF) polarity was positive, the capillary and fragment voltages were set at 1900 V and 360 V, respectively, and the gas flow rate was 5 L/min at 325°C. The spectrum was then analyzed with Agilent Mass Hunter Qualitative Analysis data acquisition software and then PEAKS Studio X software.

Database searches and bioinformatics analysis

PEAKS Studio X software was used to process data and identify proteins against an organism-specific database (Uniprot taxa: Rat). Carbamidomethylation was used as a fixed modification with a maximum of 2 cleavages. The enzyme used for digestion was trypsin. To filter out false protein matches, a false discovery rate (FDR) (1%) and a protein score (10lgP >20) were utilised. The proteins that differentially expressed among the groups were identified using label-free quantification (LFQ) in PEAKS Studio X software. Fold change ratios were calculated for protein expression by comparing treatment groups to normal control (NC) group. Proteins with fold change ≥1.20 or ≤0.83 were up-regulated or down-regulated, respectively (28). The proteins identified in the samples were assigned to respective gene symbols based on functional annotations. This was done using the Protein Analysis through Evolutionary Relationships (PANTHER) developed by UniProt. The website for PANTHER is http://www.pantherdb.org/. The dataset was analysed in order to classify the proteins based on their molecular function (MF), associated biological process (BP), and protein families. The software STRING (https://string-db) was used to construct a functional association network of possibly interacting proteins. The pathways classification was carried out following the automatic enrichment in STRING using information from the KEGG-Pathway Database.

Statistical analysis

All the data was examined using one-way analysis of variance (ANOVA) between groups and Tukey's post hoc tests. For all experiments, the significance level was fixed at $p<0.05$. SPSS version 26 was used to analyse all samples. The protein profiles were examined in each group with three replicates (n=3) to discover differences in protein profiles. PEAKS Label-Free Quantification was used to detect protein expression differences across groups with $p<0.05$. The False Discovery Rate for the Reactome pathway enrichment study was adjusted to less than 0.05.

RESULTS

Phytochemicals identification of EAMMS extract by LC-QToF-MS

The LC-QToF-MS profiling of EAMMS extract has exposed the occurrence of a total of 20 different secondary metabolites; 8 in negative ionization mode and 12 in positive ionization mode (Table I, Fig. 1). The abundance of theobromine, ishwarol, pyrimidine, 4-p-coumaroylquinic acid, pheophorbides have been identified as major bioactives compounds in EAMMS extract.

Table I: Identification of EAMMS extract by LC-QToF-MS analysis in positive and negative modes.

Cpd No.	RT (min)	Base Peak ESI - (m/z)	Base Peak ESI + (m/z)	Compound (Cpd)	Formula	Mass	Abundance ($x10^5$)
1	0.643	215.03		Theobromine	$C_7 H_8 N_4 O_2$	180.07	5.756
2	0.701	149.05		1-Methylhypoxanthine	$C_6 H_6 N_4 O$	150.05	1.229
3	0.861		205.07	Lathyrine	$C_7 H_{10} N_4 O_2$	182.08	1.994
4	1.033	115.01		Pyrimidine	$C_4 H_4 N_2$	80.04	3.584
5	9.238		499.12	3,4-Dicaffeoyl-1,5-quinolactone	$C_{25} H_{22} O_{11}$	498.12	1.439
6	9.274		479.12	Laricitrin 3-rhamnoside	$C_{22} H_{22} O_{12}$	478.11	1.524
7	9.393	337.09		4-p-Coumaroylquinic acid	$C_{16} H_{18} O_8$	338.10	2.732
8	9.396	291.09		Dihydromikanolide	$C_{15} H_{16} O_6$	292.09	1.996
9	9.415	515.12		Formononetin 7-O-glucoside-6''-O-malonate	$C_{25} H_{24} O_{12}$	516.13	1.137
10	11.381	392.23		Ile Leu Leu	$C_{18} H_{35} N_3 O_4$	357.26	1.135
11	13.201		203.18	(Z)-1,5-Tridecadiene	$C_{13} H_{24}$	180.19	1.469
12	15.523		279.23	9Z,12Z,15E-octadecatrienoic acid	$C_{18} H_{30} O_2$	278.22	1.087
13	16.086		163.08	8Z-Decene-4,6-diynoic acid	$C_{10} H_{10} O_2$	162.07	1.541
14	16.096		295.23	α-9(10)-EpODE	$C_{18} H_{30} O_3$	294.22	4.024
15	16.097		277.22	5Z,8Z,11Z,14Z-octadecatetraenoic acid	$C_{18} H_{28} O_2$	276.21	1.283
16	16.58		739.35	Normammein	$C_{21} H_{26} O_5$	358.18	1.621
17	17.023		221.19	Ishwarol	$C_{15} H_{24} O$	220.18	5.619
18	18.138		377.27	1-Linoleoyl Glycerol	$C_{21} H_{38} O_4$	354.28	2.081
19	18.162		607.26	Pheophorbide b	$C_{35} H_{34} N_4 O_6$	606.25	1.865
20	19.623	591.26		Pheophorbide a	$C_{35} H_{36} N_4 O_5$	592.27	1.399

EAMMS=ethyl acetate of *Mikania micrantha* stems extract; LC-QTOF-MS=liquid chromatography quadrupole time-of-flight mass spectrometry; RT=retention time; ESI= electrospray ionization. Ion polarity was set at negative and positive, and the mass range was from 100 – 3200 m/z. Abundance represents the relative concentration of each compounds

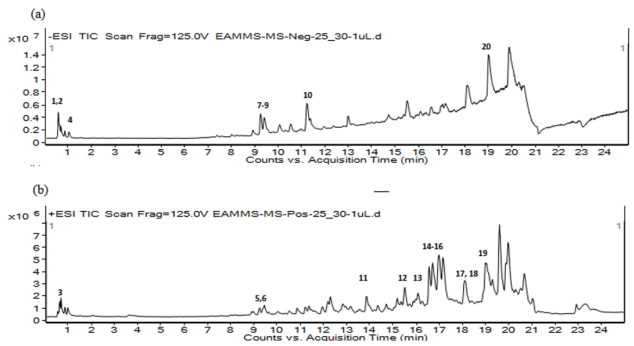

Fig. 1: (a) Mass spectrometry total ions chromatography of ethyl acetate of EAMMS extract in negative ionisation mode. (b) Mass spectrometry total ions chromatography of ethyl acetate of EAMMS extract in positive ionisation mode.

Proteomic analysis

The downregulated proteins involved in lipid metabolism and pathogenesis of hypercholesterolemia in the treatment groups were listed as Uniprot protein ID, such as, 3-hydroxy-3-methylglutaryl coenzyme A synthase, P22791; Acetyl-CoA acetyltransferase, P17764; Acyl-CoA-binding protein, P11030; Acyl-coenzyme A oxidase, F1LNW3; Long-chain specific acyl-CoA dehydrogenase, P15650 (Table II, Fig. 2). Meanwhile, the following upregulated proteins by Uniprot protein ID: Glutathione S-transferase Mu 2, P08010; Peroxiredoxin-1, Q63716; Peroxiredoxin-5, Q9R063; Regucalcin, Q03336 and Thioredoxin, P11232 (Table II, Fig. 2).

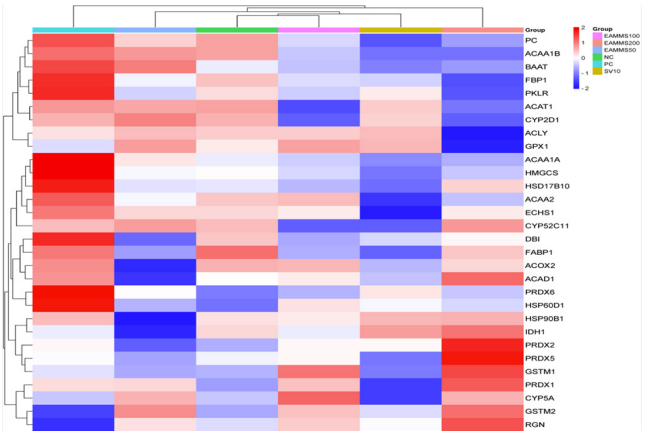

Fig. 2: Expression of proteins of control and all treated experimental rats at week 8. Heat maps displaying the changes in protein expression across controls and samples. The red color signifies the upregulation of protein expression while the blue color signifies downregulation of protein expression.

Table II: A proteomic analysis of molecular changes on liver tissues after treatment with EAMMS extract and simvastatin (SV) at week 8.

No	Name of Protein	UniProt ID	Fold Changes of Untreated Control		Fold Changes Between Control and EAMMS treatment			
			NC	PC	SV	EAMMS50	EAMMS100	EAMMS200
1	3-hydroxy-3-methylglutaryl coenzyme A synthase	P22791	1.00	1.74 (↑)	0.57 (↓)	0.97	0.88	0.83 (↓)
2	3-hydroxyacyl-CoA dehydrogenase type-2	O70351	1.00	1.65 (↑)	0.68 (↓)	0.99	0.88	1.17
3	3-ketoacyl-CoA thiolase	P13437	1.00	1.18	0.57 (↓)	0.90	1.02	0.82 (↓)
4	3-ketoacyl-CoA thiolase A	P21775	1.00	1.73 (↑)	0.72 (↓)	1.11	0.92	0.83 (↓)
5	3-ketoacyl-CoA thiolase B	P07871	1.00	1.09	0.56 (↓)	1.02	0.72 (↓)	0.56 (↓)
6	Acetyl-CoA acetyltransferase	P17764	1.00	1.02	0.91	0.99	0.42 (↓)	0.52 (↓)
7	Acyl-CoA-binding protein	P11030	1.00	1.14	0.92	0.82 (↓)	0.88	0.96
8	Acyl-coenzyme A oxidase	F1LNW3	1.00	1.07	0.71 (↓)	0.40 (↓)	0.99	0.92
9	ATP-citrate synthase	P16638	1.00	0.92	1.05	1.05	0.99	ND
10	Bile acid-CoA:amino acid N-acyltransferase	Q63276	1.00	1.15	0.92	1.11	0.97	0.94
11	Cytochrome b5	P00173	1.00	1.00	ND	1.88 (↑)	2.40 (↑)	1.88 (↑)
12	Cytochrome P450 2C11	P08683	1.00	1.00	ND	1.13	ND	1.14
13	Cytochrome P450 2D1	P10633	1.00	1.00	0.87	1.19	ND	ND
14	Enoyl-CoA hydratase	P14604	1.00	1.33 (↑)	ND	1.00	0.92	0.92
15	Fatty acid-binding protein	P02692	1.00	0.99	0.69 (↓)	0.75 (↓)	0.77 (↓)	0.91
16	Fructose-1 6-bisphosphatase 1	P19112	1.00	1.27 (↑)	0.82 (↓)	0.87	0.84	0.58 (↓)
17	Glutathione peroxidase 1	P04041	1.00	0.79 (↓)	1.20 (↑)	1.30 (↑)	1.28 (↑)	ND
18	Glutathione S-transferase Mu 1	P04905	1.00	1.08	0.90	0.98	1.36 (↑)	1.44 (↑)
19	Glutathione S-transferase Mu 2	P08010	1.00	0.89	1.05	1.20 (↑)	1.15	1.23 (↑)
20	Heat shock protein HSP 90-beta	P34058	1.00	1.13	1.15	ND	0.97	1.17
21	Heat shock protein 60	P63039	1.00	1.11	1.04	1.02	1.05	1.03
22	Isocitrate dehydrogenase [NADP]	P41562	1.00	0.96	1.04	0.81 (↓)	0.96	1.07
23	Long-chain specific acyl-CoA dehydrogenase	P15650	1.00	1.14	0.92	0.72 (↓)	1.02	1.19
24	Peroxiredoxin-1	Q63716	1.00	1.14	0.88	1.15	1.17	1.29 (↑)
25	Peroxiredoxin-2	P35704	1.00	1.05	1.05	0.95	1.05	1.18
26	Peroxiredoxin-5	Q9R063	1.00	1.01	0.90	0.94	1.02	1.20 (↑)
27	Peroxiredoxin-6	O35244	1.00	1.19	1.08	1.07	1.03	1.04
28	Pyruvate carboxylase	P52873	1.00	1.18	0.43 (↓)	0.90	0.72 (↓)	0.60 (↓)
29	Pyruvate kinase	P12928	1.00	1.37 (↑)	0.96	0.83 (↓)	0.82 (↓)	0.57 (↓)
30	Regucalcin	Q03336	1.00	0.65 (↓)	1.06	1.12	1.16	1.40 (↑)
31	Superoxide dismutase-1	P07632	1.00	1.19	0.99	0.86	0.86	1.02
32	Thioredoxin-1	P11232	1.00	1.32 (↑)	1.23 (↑)	1.18	1.43 (↑)	1.87 (↑)

ND: Not determine; upregulation (threshold values of ≥1.20) and downregulation (threshold values of ≤0.83) of the protein are represented as (↑) and (↓), respectively. The data were compared to one another using PEAKS Q. The N number for all controls and samples is three, and the p-value is set at 0.05.

Biological process, molecular function and protein network interaction of differential expressed proteins

Fig. 3 depicts the biological process and molecular functions of the proteins that have exhibited differential expression. The proteins that exhibited dysregulation following treatment with EAMMS extract, as compared to the control group, were categorised based on their involvement in specific biological processes and their molecular functions using the Panther online database (http://pantherdb.org). In relation to the categorization of biological processes, it is observed that the largest proportion of differentially expressed proteins is associated with cellular processes (37.9%). This is followed by response to stimulus (16.7%), biological regulation (7.6%), metabolic processes (3.3%), immune system processes (3.0%), and localisation (1.5%), as visually represented in Fig. 3 (A). As shown in Fig. 3 (B), the distribution of differentially expressed proteins according to their molecular function indicates that exposure to EAMMS extract dysregulates primarily proteins with catalytic activity (70%) and binding proteins (30%).

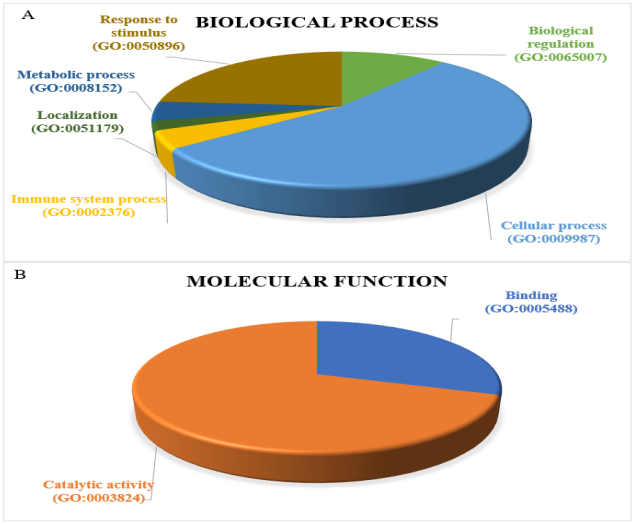

Fig. 3: Panther Gene Ontology classification of the differentially expressed proteins in the liver of Sprague Dawley rats exposed to the treatment of EAMMS extract compared to control group according to (A) biological process and (B) molecular function.

As shown in Fig. 4, a total of 30 nodes are linked together by 46 interactions in the PPI network, some of which are narrow and dense. The protein interaction networks exhibited a significant enrichment, as indicated by the statistical value of 0.0137. Furthermore, STRING software was used to obtain the KEGG-Pathway Enrichment to investigate biomolecular pathway maps (Table III) such as lipid metabolism, amino acid metabolism and biosynthesis, pyruvate metabolism and glutathione metabolism.

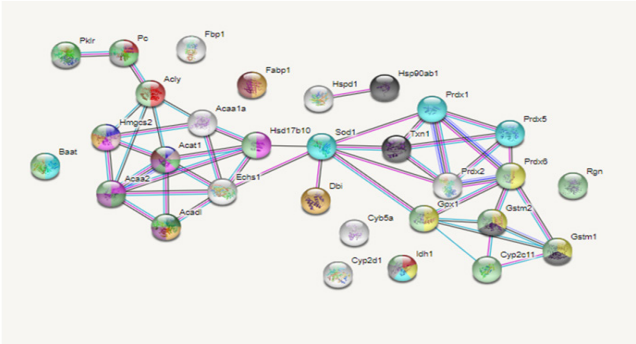

Fig. 4: Protein-protein interaction network obtained by STRING software. Different colored edges represent the existence of different type of evidence. A green line indicates neighbourhood evidence; a blue line, gene co-occurance; a purple line, experimental evidence; a black line, co-expression. ACAT1, Acetyl-CoA acetyltransferase; ACAA2, Acetyl-coa acyltransferase 2; ACAA1A, 3-ketoacyl-CoA thiolase A; ACAA1B, 3-ketoacyl-CoA thiolase B; ACLY, ATP-citrate synthase; FABP1, Fatty acid-binding protein; HMGCS2, 3-hydroxy-3-methylglutaryl-CoA synthase; HSPD1, 60 kDa heat shock protein; HSP90AB1, Heat shock protein 90; PRDX1, Peroxiredoxin-1; RGN, Regucalcin; BAAT, Bile acid-CoA:amino acid N-acyltransferase; CYB5A, Cytochrome b5; CYP2C11, Cytochrome P450 2C11; CYP2D1, Cytochrome P450 2D1; ECHS1, Enoyl-CoA hydratase; FBP1, Fructose 1,6-biphosphatase 1; GPX1, Glutathione peroxidase 1; GSTM1, Glutathione S-transferase Mu 1; GSTM2, Glutathione S-transferase Mu 2; IDH1, Isocitrate dehydrogenase [NADP] cytoplasmic; ACADL, Long-chain specific acyl-CoA dehydrogenase; PRDX1, Peroxiredoxin-1; PRDX2, Peroxiredoxin-2; PRDX5, Peroxiredoxin-5; PRDX6, Peroxiredoxin-6; PC, Pyruvate carboxylase; PKLR, Pyruvate kinase; RGN, Regucalcin; TXN1, Thioredoxin.

Table III: KEGG-Analysis using STRING software yielded a list of established pathways and the number of proteins involved based on Figure 4.

KEGG Pathways	Count in Network
Fatty acid metabolism	3
Fatty acid degradation	3
Fat digestion and absorption	2
Fluid shear stress and atherosclerosis	4
Biosynthesis of amino acids	3
PPAR signalling pathway	4
Pyruvate metabolism	3
Citrate/TCA cycle	3
Glutathione metabolism	5
Metabolic pathways	16

DISCUSSION

The current investigation demonstrated that the administration of EAMMS treatment resulted in the reduction of expression levels of both acetyl-CoA acetyltransferase (ACAT1) and acetyl-CoA acetyltransferase 2 (ACAT2). ACAT1 plays a role in the production of macrophage foam cells, whereas ACAT2 is involved in the process of cholesterol esterification which converting free cholesterol into cholesterol ester, as well as intestinal cholesterol absorption, and the release of lipoproteins containing ApoB (29,30). In a previous study, Repa et al. (31) reported that the inhibition of ACAT2 has been shown to effectively suppress cholesterol absorption and decrease levels of fat. Ibrahim et al. (6) reported that the administration of EAMMS extract resulted in the most significant inhibition of the enzymes HMGCR and ACAT2 in rats, when compared to the control group. From phytochemical analysis, the presence of pheophorbides in the EAMMS extract could be attributed to the extracts' ability to reduce ACAT activity. Song et al. found that pheophorbides inhibited ACAT activity with the IC50 value of 1.1 ug/mL in an enzyme assay using rat liver microsome with a dose dependent fashion (31). Pheophorbides have also been demonstrated to inhibit lipid accumulation by suppressing SREBP-1-mediated lipogenesis in the liver. Lessening of ACAT activity serves as a target for the treatment of hypercholesterolemia and atherosclerosis progression (32).

The protein expressions associated with lipid biosynthesis include hydroxymethylglutaryl-CoA synthase cytoplasmic (HMGCS2), which serves as the initial enzyme in the mevalonate biosynthesis pathway and acts as a precursor for sterol isoprenoids, including cholesterol (33). According to De Rosa et al. (34), high cholesterol concentrations in the liver significantly increased HMGCS2 gene expression. Overexpression of this protein in the liver of rats because of a saturated fat-rich diet. EAMMS treatment attenuated the protein expression of HMGCS2 at a dosage of 200 mg/kg. The

anti-hypercholesterolemic potency of EAMMS extract due to the high phenolic acids and flavonoid contents in *Mikania micrantha* (15,35) which have also showed antihypercholesterolemic effects in other plant extracts.

The implementation of a high cholesterol diet at a concentration of 1% resulted in a decrease in the expression levels of proteins associated with lipid metabolism, including Glutathione S-transferase Mu 2 (GSTM2), in comparison to normal rats. However, treated rats with EAMMS extract at 50 mg/kg and 200 mg/kg revealed the extract's ability to increase GSTM2 expression in the rats. These findings could be attributed to the effects of bioactive compounds found in *M. micrantha* on GSTM2 protein expression. GSTM2 expression, according to Lan et al. (36), could attenuate lipid accumulation and inflammation. Furthermore, GSTM2 has been shown to regulate abnormal lipid metabolism in a variety of pathological processes (37).

The results show that EAMMS extract exposure increased the expression of Thioredoxin-1 (TRX-1) at dosages of 100 mg/kg and 200 mg/kg (Table II). Thioredoxin-1 (TRX-1) is a 12-kDa highly conserved protein that, along with TRX-1 reductase and NADPH, functions as a regulator of cellular reduction/oxidation (38). Previous research has shown that TRX-1 and polyphenols play crucial roles in cardiovascular system protection, including anti-oxidative and anti-inflammatory functions (39-41). Therefore, the effect of EAMMS extract had imposed as anti-hypercholesterolemic activities on regulating the activity of TRX-1, which could be an alternative target for treating hypercholesterolemia and atherosclerosis. Also, EAMMS treatment of rats at a dose of 200 mg/kg demonstrated the ability to upregulate the expression of PRDX1 and PRDX5. This evidence suggested that EAMMS extract, which contains abundance of bioactive compound such as theobromine decreased the PRDXs expression. This study is supported with a previous study by Janitschke et al. (42), who discovered this alkaloid upregulated the expression of PRDX1 and PRDX5 in rats. Hence, this reaction suggested that EAMMS extract could protect cholesterol homeostasis from oxidative stress and reduce the risk of CVD.

Phenolic compounds may contribute to improving endogenous antioxidant defense by restoring or augmenting the activities of antioxidant enzymes glutathione peroxidase (GPX1) and, as a result, glutathione content (43). The proteins encoded by GPX1 from glutathione metabolism are involved in the detoxification of hydrogen peroxide and lipid hydroperoxides respectively and are the most important antioxidant enzymes. Glutathione peroxidases 1 (GPX1) was upregulated in the rats treated with EAMMS extract (50 mg/kg and 100 mg/kg). The results are consistent with the gene expression of GPX1 in a previous study, which discovered that feeding mice a theobromine-rich diet for 20 days can stimulate Nrf2 activation and, as consequently, increase the expression of both superoxide dismutase (SOD-1) and GPX by its own (44). Additionally, the levels of expression of SOD-1 also were found to be higher in the group treated with EAMMS extract. The enzyme, which is encoded by SOD-1, destroys free superoxide radicals in tissues. In addition, EAMMS extract raised the expression of isocitrate dehydrogenase 1 (NADPH), which is involved in the regeneration of NADPH for antioxidant systems, which provides hydroquinone as an antioxidant (45).

Besides, rats treated with EAMMS extract at high doses of 100 mg/kg and 200 mg/kg showed the ability to down-regulate the expression of pyruvate carboxylase, which can prevent lipid formation at the start of lipid synthesis pathways. These findings suggest that polyphenols in *M. micrantha* have the potential to act as pyruvate carboxylase inhibitors, which is in line with the findings of other authors (46). Other than that, EAMMS exposure up regulated the expression of regucalcin at dosage of 200 mg/kg. Regucalcin is essential for controlling lipid and glucose metabolism (47). According to Yamaguchi and Nakagawa (48), total cholesterol, free fatty acids, hepatic triglycerides, and glycogen were reduced in regucalcin in TG rats. Besides, regucalcin had inhibited the activation of cytoplasmic pyruvate kinase, and fructose 1,6-diphosphatase in rat liver. These results are consistent with this proteomic analysis's finding that the expression of fructose 1,6-diphosphatase and pyruvate kinase were suppressed by up-regulation of regucalcin (49).

The present findings also provide strong evidence that the use of EAMMS extract may be attributable to the up-regulation of protein involved in glutathione metabolism, such as GPX1, GSTM1 and GSTM2, which play crucial roles in antioxidant defence and the regulation of cellular events, as well as TRX1, which contributes to cellular redox balance. Also, down-regulation of lipid and fatty acid metabolism proteins such as HMGCS2, ACAT1, ACLY, FABP1 may contribute to the possible mechanism for EAMMS extract's cholesterol-lowering effect.

Further study employing preclinical studies and controlled trials is required to investigate the limitations of the medications in conjunction with EAMMS extract as new drug delivery vehicles. In addition to lifestyle modification, pharmacotherapy and individualized treatment regimens remain the primary pillars of hypercholesterolemia and other metabolic-syndrome-related disorders. Furthermore, because rats and humans have different anatomy, gene expression, cholesterol metabolism, and clinical translatability (50), this study provides new insights into the mechanism of action of EAMMS extract on cholesterol metabolism and expands the rat model's utility for translational research in

hypercholesterolemia.

CONCLUSION

A wide range of secondary metabolites which are present in *M. micrantha* demonstrated promising therapeutic properties EAMMS extract. The identified compounds such as theobromine, ishwarol, pyrimidine, 4-p-coumaroylquinic acid, pheophorbides and dihydromikanolide suggested bioactive compound that contributed to cholesterol-lowering properties of EAMMS extract. The proteomic data revealed more information about the metabolic pathways modulated by EAMMS extract, implying the underlying mechanisms by which *M. micrantha* extracts regulate protein expression to potentially lowering the cholesterol and thereby prevent the cardiovascular diseases (CVDs), which is mainly through the regulation of proteins involved in lipid metabolism pathways. In conclusion, this study demonstrated the potential anti-hypercholesterolemic effects of *M. micrantha* and provide understanding on the molecular targets of EAMMS extract, which could be used for further clinical study on the putative anti-hypercholesterolemic properties.

ACKNOWLEDGEMENT

The authors would like to acknowledge the Universiti Putra Malaysia, Malaysia for providing the laboratory facilities and financing the project (research university grant: GP-IPM/2017/9524500).

REFERENCES

1. Adekiya TA, Shodehinde SA, Aruleba RT. Anti-hypercholesterolemic effect of unripe *Musa paradisiaca* products on hypercholesterolemia-induced rats. J Appl Pharm Sci. 2018;8(10):90-7. doi: 10.7324/JAPS.2018.81012.
2. Avcı G, Kupeli E, Eryavuz A, Yesilada E, Kucukkurt I. Antihypercholesterolaemic and antioxidant activity assessment of some plants used as remedy in Turkish folk medicine. J Ethnopharmacol. 2006;107(3):418-23. doi: 10.1016/j.jep.2006.03.032.
3. Das SS, Vasisht S, Das N, Srivastava LM, Dubey KK, Watal G. Correlation between total antioxidant status and lipid peroxidation in hypercholesterolemia. Curr Sci -Bangalore. 2000;78(4):486-86.
4. Aftab T, Hakeem KR. Medicinal and Aromatic Plants: Healthcare and Industrial Applications. Springer Nature. 2021. doi:10.1007/978-3-030-58975-2_1.
5. Sham TT, Chan CO, Wang YH, Yang JM, Mok DK, Chan SW. A review on the traditional Chinese medicinal herbs and formulae with hypolipidemic effect. Biomed Res Int. 2014:1-21. doi: 10.1155/2014/925302.
6. Ibrahim A, Shafie NH, Mohd Esa N, Shafie SR, Bahari H, Abdullah MA. *Mikania micrantha* extract inhibits HMG-CoA reductase and ACAT2 and ameliorates hypercholesterolemia and lipid peroxidation in high cholesterol-fed rats. Nutrients. 2020;12(10):3077-3086. doi: 10.3390/nu12103077.
7. Bellosta S, Paoletti R, Corsini A. Safety of statins: Focus on clinical pharmacokinetics and drug interactions. Circulation 2004, 109, 50-57. https://doi.org/10.1161/01.CIR.0000131519.15067.1f
8. Day MD, Clements DR, Gile C, Senaratne WK, Shen S, Weston LA, Zhang F. Biology and impacts of Pacific Islands invasive species. *Mikania micrantha* Kunth (Asteraceae). Pac Sci. 2016;70(3):257-85. doi: 10.2984/70.3.1.
9. Tripathi RS, Khan ML, Yadav AS. Biology of *Mikania micrantha* HBK: A review. Invasive alien plants: An ecological appraisal for the Indian subcontinent. 2012;9(10):99-107.
10. Saha S, Mandal SK, Chowdhury HR. Anato-pharmacognostic studies of *Mikania micrantha* Kunth: a promising medicinal climber of the family Asteraceae. Int J Res Ayurveda Pharm. 2015;6(6):773-80. doi: 10.7897/2277-4343.066144.
11. Ardianto A, Munarsih D, Rahayu IN, Aslam MM, Aditya MF, Estiningsih D, Fatmawati A, Saputro PH. Screening, and antidiarrheal activity testing of Sembung Rambat (*Mikania micrantha*) leaves. J Med Sci. 2022;10(8):194-9. doi: 10.3889/oamjms.2022.9458.
12. Nurdiana S, Nur Ajeerah S, Nur Farhana AS, Siti Khairiyah MH, Norashirene MJ. Hypoglycaemic, antioxidant and wound healing activities of *Mikania micrantha* leaves extract in normal and alloxan-induced diabetic rats. Focus and Scope. 2013;7(2):6-10. doi: 10.22159/ajpcr.2018.v11i3.23283.
13. Deori C, Dutta G, Das S, Phukan D, Gogoi G. To evaluate the anti-inflammatory activity of ethanolic extract of leaves of *Mikania micrantha* on experimental animal models. J Evol Med Dent Sci. 2017;6(50):3818-22.
14. Chetia J, Upadhyaya S, Bora DK. Screening of phytochemicals, antioxidant, and antimicrobial activity of some tea garden weeds of Tinsukia, Assam. Int J Pharm Sci Rev Res. 2014;26(33):193-6.
15. Ishak AH, Shafie NH, Esa NM, Bahari H, Ismail A. From weed to medicinal plant: Antioxidant capacities and phytochemicals of various extracts of *Mikania micrantha*. Int J Agric Biol; 2018;20(3):561-8. doi: 10.17957/IJAB/15.0522.
16. Wan Nurhayati WH, Norli Arlizan T, Nurdiana S. Effect of *Mikania micrantha* leaf extract on the level of blood glucose and hepatic glycogen in the normal and alloxan-induced diabetic rats. Indian J Nat Prod Resour. 2013;9(10):398-402.

17. Matawali A, Chin LP, Eng HS, Boon LH, Gansau JA. In vitro evaluation of antikinase, antiphosphatase and cytotoxic activities of *Mikania micrantha* HBK (Asteraceae) from Malaysia. J Chem Pharm Sci. 2016;9(2):696-701.
18. Dou X, Zhang Y, Sun N, Wu Y, Li L. The anti-tumor activity of *Mikania micrantha* aqueous extract in vitro and in vivo. Cytotechnology. 2014;66(1):107-17. doi: 10.1007/s10616-013-9543-9.
19. Ríos E, León A, Chávez MI, Torres Y, Ramírez-Apan MT, Toscano RA, *et al*. Sesquiterpene lactones from *Mikania micrantha* and *Mikania cordifolia* and their cytotoxic and anti-inflammatory evaluation. Fitoterapia. 2014;94(1):155-63. doi: 10.1016/j.fitote.2014.02.006.
20. Jyothilakshmi M, Jyothis M, Latha MS. Antidermatophytic activity of *Mikania micrantha* Kunth: an invasive weed. Pharmacognosy Res. 2015;7(1):20-1. doi: 10.4103/0974-8490.157994.
21. Mc PA, Ocotero VM, Balcazar RI, Jiménez FG. Phytochemical and pharmacological studies on *Mikania micrantha* HBK (Asteraceae). Phyton. 2010;79(1):77-77. doi: 10.32604/phyton.2010.79.077.
22. Dev UK, Hossain MT, Islam MZ. Phytochemical investigation, antioxidant activity and anthelmintic activity of *Mikania micrantha* leaves. World J Pharm Res. 2015;4(5):121-33.
23. Gómez MJ, Gómez-Ramos MM, Malato O, Mezcua M, Férnandez-Alba AR. Rapid automated screening, identification and quantification of organic micro-contaminants and their main transformation products in wastewater and river waters using liquid chromatography–quadrupole-time-of-flight mass spectrometry with an accurate-mass database. J of Chromatography A. 2010;1217(45):7038-54.
24. Gianazza E, Zoanni B, Mallia A, Brioschi M, Colombo GI, Banfi C. Proteomic studies on apoB-containing lipoprotein in cardiovascular research: A comprehensive review. Mass Spect. Rev. 2023;42(4):1397-423.
25. Huang C, Zhang J, Huang J, Li H, Wen K, Bao J, Wu X, Sun R, Abudukeremu A, Wang Y, He Z. Proteomic and functional analysis of HDL subclasses in humans and rats: a proof-of-concept study. Lipids in Health Dis. 2023; 29;22(1):86-88.
26. Lee CH. A simple outline of methods for protein isolation and purification. Endocrinol Metab. 2017;32(1):18-22. doi: 10.3803/EnM.2017.32.1.18.
27. Hishamuddin MS, Lee SY, Isa NM, Lamasudin DU, Abidin SA, Mohamed R. Time-based LC-MS/MS analysis provides insights into early responses to mechanical wounding, a major trigger to agarwood formation in *Aquilaria malaccensis* Lam. RSC Adv. 2019;9(32):18383-93. doi: 10.1039/C8RA10616A.
28. Meng S, Xia W, Pan M, Jia Y, He Z, Ge W. Proteomics profiling and pathway analysis of hippocampal aging in rhesus monkeys. BMC Neurosci. 2020;21(1):1-2. doi: 10.1186/s12868-020-0550-4.
29. Dove DE, Su YR, Swift LL, Linton MF, Fazio S. ACAT1 deficiency increases cholesterol synthesis in mouse peritoneal macrophages. Atherosclerosis. 2006;1;186(2):267-74. doi: 10.1016/j.atherosclerosis.2005.08.005.
30. Borradaile NM, de Dreu LE, Barrett PH, Huff MW. Inhibition of hepatocyte apoB secretion by naringenin. J Lipid Res. 2002;43(9):1544-54. doi: 10.1194/jlr.M200115-JLR200.
31. Repa JJ, Buhman KK, Farese Jr RV, Dietschy JM, Turley SD. ACAT2 deficiency limits cholesterol absorption in the cholesterol-fed mouse: Impact on hepatic cholesterol homeostasis. Hepatology. 2004;40(5):1088-97. doi: 10.1002/hep.20439.
32. Pal P, Gandhi H, Giridhar R, Yadav MR. ACAT inhibitors: the search for novel cholesterol lowering agents. Min-Rev Med Chem. 2013;13(8):1195-1219. doi: 10.2174/1389557511313080007.
33. Sapir A, Tsur A, Koorman T, Ching K, Mishra P, Bardenheier A, *et al*. Controlled sumoylation of the mevalonate pathway enzyme HMGS-1 regulates metabolism during aging. Proc Natl Acad Sci. 2014;111(37):3880-9. doi: 10.1073/pnas.1414748111.
34. De Rosa MC, Caputo M, Zirpoli H, Rescigno T, Tarallo R, Giurato G, *et al*. Identification of genes selectively regulated in human hepatoma cells by treatment with dyslipidemic sera and PUFAs. J Cell Physiol. 2015;230(9):2059-66. doi: 10.1002/jcp.24932.
35. Rescigno T, Capasso A, Tecce MF. Involvement of nutrients and nutritional mediators in mitochondrial 3-hydroxy-3-methylglutaryl-CoA synthase gene expression. J Cell Physiol. 2018;233(4):3306-14. doi: 10.1002/jcp.26177.
36. Lan T, Hu Y, Hu F, Li H, Chen Y, Zhang J, *et al.* Hepatocyte glutathione S-transferase mu 2 prevents non-alcoholic steatohepatitis by suppressing ASK1 signaling. J Hepatol. 2022;76(2):407-19. doi: 10.1016/j.jhep.2021.09.040.
37. Chen C, Wen M, Wang C, Yuan Z, Jin Y. Differential proteomic analysis of mouse cerebrums with high-fat diet (HFD)-induced hyperlipidemia. Peer J. 2022;10:e13806. doi: 10.7717/peerj.13806.
38. Lu J, Holmgren A. The thioredoxin antioxidant system Free Radic Biol Med. 2014;66:75-87. doi: 10.1016/j.freeradbiomed.2013.07.036.
39. Namba F, Kobayashi-Miura M, Goda T, Nakura Y, Nishiumi F, Son A, *et al*. Human thioredoxin-1 attenuates the rate of lipopolysaccharide-induced preterm delivery in mice in association with its anti-inflammatory effect. Pediatr Res. 2016;80(3):433-9. doi: 10.1038/pr.2016.100.
40. Watanabe R, Nakamura H, Masutani H, Yodoi J. Anti-oxidative, anti-cancer, and anti-inflammatory actions by thioredoxin 1 and thioredoxin-binding

protein-2. Pharmacol Ther. 2010;127(3):261-70. doi: 10.1016/j.pharmthera.2010.04.004.
41. Mosele F, Tavares AM, Colombo R, Caron-Lienert R, Araujo AS, Ribeiro MF, et al. Effects of purple grape juice in the redox-sensitive modulation of right ventricular remodeling in a pulmonary arterial hypertension model. J Cardiovasc Pharmacol. 2012;60(1):15-22. doi: 10.1097/FJC.0b013e3182550fd6.
42. Janitschke D, Lauer AA, Bachmann CM, Seyfried M, Grimm HS, Hartmann T, et al. Unique role of caffeine compared to other methylxanthines (theobromine, theophylline, pentoxifylline, propentofylline) in regulation of ad relevant genes in neuroblastoma sh-sy5y wild type cells. Int J Mol Sci. 2020;21(23):9015-9018. doi: 10.3390/ijms21239015.
43. Toufektsian MC, de Lorgeril M, Nagy N, Salen P, Donati MB, Giordano L, *et al.* Chronic dietary intake of plant-derived anthocyanins protects the rat heart against ischemia-reperfusion injury. J Nutr. 2008;138(4):747-52. doi: 10.1093/jn/138.4.747.
44. Fernández-Fernández L, Esteban G, Giralt M, Valente T, Bolea I, Solé M, et al. Catecholaminergic and cholinergic systems of mouse brain are modulated by LMN diet, rich in theobromine, polyphenols and polyunsaturated fatty acids. Food & Func. 2015;6(4):1251-60. doi: 10.1039/C5FO00052A.
45. Azevedo Martins TE, Sales de Oliveira Pinto CA, Costa de Oliveira A, Robles Velasco MV, Gorriti Guitiérrez AR, Cosquillo Rafael MF, *et al.* Contribution of topical antioxidants to maintain healthy skin—A review. Sci Pharma. 2020;88(2):27. doi: 10.3390/scipharm88020027.
46. Donado-Pestana CM, dos Santos-Donado PR, Daza LD, Belchior T, Festuccia WT, Genovese MI. Cagaita fruit (Eugenia dysenterica DC.) and obesity: Role of polyphenols on already established obesity. Food Res Int. 2018;103:40-7. doi: 10.1016/j.foodres.2017.10.011.
47. Yamagishi K, Iso H, Kokubo Y, Saito I, Yatsuya H, Ishihara J, *et al.* Dietary intake of saturated fatty acids and incident stroke and coronary heart disease in Japanese communities: the JPHC Study. Eur Heart J. 2013;34(16):1225-32. doi: 10.1093/eurheartj/eht043.
48. Yamaguchi M, Nakagawa T. Change in lipid components in the adipose and liver tissues of regucalcin transgenic rats with increasing age: suppression of leptin and adiponectin gene expression. Int J Mol Med. 2007;20(3):323-8. doi: 10.3892/ijmm.20.3.323.
49. Yamaguchi M. Regucalcin and cell regulation: role as a suppressor protein in signal transduction. Mole Cell Biochem. 2011;353(1):101-37. doi: 10.1007/s11010-011-0779-4.
50. Van de Steeg E, Kleemann R, Jansen HT, van Duyvenvoorde W, Offerman EH, Wortelboer HM, DeGroot J. Combined analysis of pharmacokinetic and efficacy data of preclinical studies with statins markedly improves translation of drug efficacy to human trials. J Pharmacol Exp Ther. 2013;347(3):635-44.